Research Square

Preprints are preliminary reports that have not undergone peer review.
They should not be considered conclusive, used to inform clinical practice,
or referenced by the media as validated information.

Reaction Mechanism and Rate Constants of Benzothiophene Desulfurization: A DFT and Kinetic Modeling Study

Basheer Aazaad
Saveetha Engineering College
Angappan Mano Priya
manoophys@gmail.com

Université de Rennes - Campus de Beaulieu: Universite de Rennes

Research Article

Keywords: Sulfur compounds, benzothiophene, polycyclic aromatic compounds, OH, H2 and HO2, kinetics, branching ratios and lifetime

Posted Date: June 10th, 2026

DOI: https://doi.org/10.21203/rs.3.rs-9628562/v1

License: This work is licensed under a Creative Commons Attribution 4.0 International License.
Read Full License

REACTION MECHANISM AND RATE CONSTANTS OF BENZOTHIOPHENE DESULFURIZATION: A DFT AND KINETIC MODELING STUDY

Basheer Aazaad[1], and Angappan Mano Priya[2]*

[1] *Department of Physics, Saveetha Engineering College, Thandalam, Chennai-602105, Tamilnadu, India.*

[2] *Institut de Physique de Rennes - UMR 6251 du CNRS, Université de Rennes, Rennes, France.*

Corresponding Author: manoophys@gmail.com, mano-priya.angappan@univ-rennes.fr

ABSTRACT

Benzothiophene (BT), a promising organosulfur and heterocyclic compound, is a toxic sulfur containing polycyclic aromatic hydrocarbon pollutant which is released into the atmosphere by means of fossil fuels refining, combustion and various sources. Besides, many clinical drugs are produced based on BT and its derivative compounds, which have been widely used to treat a variety of diseases with high therapeutic efficacy. In this research article, a promising density functional theory (DFT) was selected to shed light on the addition / abstraction / auto-oxidation / desulfurization reaction mechanisms of BT with OH radical, HO_2 and H_2 oxidants. The present study is proposed with the possible reaction pathways to elucidate the detailed decomposition mechanism of BT and the elimination mechanism of H_2S. The decomposition or auto-oxidation of BT leads to the formation of desulfurization end-products, namely benzene and ethane. To further validate the proposed mechanism, kinetic calculations were performed for the OH reaction channel, and the branching ratios as well as the atmospheric lifetime of BT were subsequently determined. This is the first kinetic report for BT with OH radical and to the best of our knowledge; there are no literature report for the comparison.

Keywords: Sulfur compounds, benzothiophene, polycyclic aromatic compounds, OH, H_2 and HO_2, kinetics, branching ratios and lifetime.

INTRODUCTION

Sulfur containing compounds, particularly those fused thiophene have attracted significant attention due to their potential health hazards(Herrera et al. 2009, Li et al. 2019). Benzothiophene (BT) is a promising heterocyclic and organosulfur compound served as a suitable candidate in broad range of research fields. It comprises six membered benzene and five membered thiophene rings with molecular formula of C_8H_6S. Toxic sulfur containing polycyclic aromatic hydrocarbon pollutants are released into the atmosphere by means of fossil fuels refining, combustion and various sources are of significant interest and gaining attention particularly in environmental chemistry and organic synthesis(Qi et al. 2020). In addition, BTs are present in many biologically active compounds(Deng et al. 2021, Keri et al. 2017, Shen et al. 2020) and organic materials(Algso et al. 2018). It is well known from the literature studies; BT is used in many potent applications like organic synthesis and pharmaceutical relevance.

Despite numerous experimental and theoretical studies—such as the 2020 work by Johannes Claußnitzer *et al.* on the desulfurization of BT using molecular oxygen catalyzed by HPA-5—it was found that the organic sulfur present in BT is ultimately converted into sulfuric acid(Claußnitzer et al. 2020). Desulfurization mechanisms of thiophene and BT under inert and oxidative atmospheres by Fuli et.al(Zhang et al. 2020) in 2020 explained the mechanism of catalytic desulfurization processes. Il-Kyu Kim et.al(Kim et al. 2003) in 2003 studied about the sonochemical decomposition of BT and their kinetic analysis predicted 77% of decomposition occurred via OH radical addition. Many experimental studies have been done on BT desulfurization and decomposition, in addition to these BT pyrolysis mechanisms have been studied theoretically by Tianshuang Li et.al(Li et al. 2019) in 2019 and they predicted BT have higher thermal stability. Reaction mechanisms for hydro-desulfurization process of BT on a Mo3S9 model cluster have been investigated theoretically by Xiao-Qian

Yao et.al(Yao et al. 2005) in 2005 found that hydrogenation of BT with dihydrobenzothiophene reaction is more favoured and their results are correlated with experimental findings. Recently M. K. Prabhu et.al(Prabhu et al. 2025) in 2025 Catalytic Hydrodesulfurization of BT on a CoMoS Catalyst, their finding promotes new insight of C-S bond cleavage. Although several studies have been reported on the desulfurization of BT, there is still a lack of findings regarding its reaction mechanism with OH, H_2, and HO_2, which needs further exploration.

In the present study, our first objective was to assess the reaction mechanism of OH, H_2 and HO_2 with BT in gas and solvent phase. The reaction of BT with OH is of considerably importance in both atmospheric and combustion chemistry. Its degradation pathways lead to the formation of sulfur- and oxygen-containing secondary pollutants, and the atmospheric lifetime of BT can be theoretically determined to better understand its fate. The OH radical can attack the benzene or thiophene ring either via H-abstraction or OH addition in BT resulting in the formation of hydroxylated derivative or ring opened products. The reaction of BT with H_2 is particularly important in high-temperature combustion and industrial hydrodesulfurization (HDS) processes, where H_2 facilitates the breakdown of BT, thereby minimizing sulfur emissions from fuels. Although the reaction mechanisms of BT with OH and H_2 are important, the role of the HO_2 radical is also significant, as its reactions with BT can lead to the formation of secondary organic aerosols (SOAs), thereby influencing both local air quality and global climate. The addition of HO_2 radical can easily add to thiophene ring in BT. Understanding the reaction mechanisms of BT with OH, H_2, and HO_2 is crucial for predicting its behavior in different environments, assessing its environmental impact, and optimizing desulfurization strategies in energy applications.

COMPUTATIONAL DETAILS

Initially, the geometries of BT and all the possible titled reactants, intermediates, products were fully optimized in both gas and solvent phases using density functional theory (DFT). All the electronic structure calculations throughout the manuscript were carried out using meta-hybrid Minnesota exchange-correlation hybrid density functional (M06-2X) (Zhao &Truhlar 2008) along with 6-311++G(d,p) (Aazaad &Lakshmipathi 2018) basis set. Followed by, the harmonic vibrational frequency analysis was carried out at the same level of theory to confirm that all the energy minima are with all positive frequencies. Whereas, the first order saddle point on the potential energy surface (PES) were characterized with only one imaginary frequency (NIMF = 1). Further, to validate the results obtained at the DFT theory (M06-2X), all the molecular entities were re-optimized at the second order Møller-Plesset Perturbation Theory (MP2/6-311++G(d,p) level of theory. These calculations were carried out in both gas phase and solvent phase (water) to ensure consistency and accuracy of the predicted reaction mechanism and energetics.

The solvent effects were included using the Integral Equation Formalism Polarizable Continuum Model (IEFPCM) with water as the solvent, as implemented in Gaussian (Lipparini et al. 2010, Marenich et al. 2009, Miertuš et al. 1981, Scalmani &Frisch 2010). Water was chosen as the solvent to simulate a polar reaction environment and to account for solvation effects on the stability of intermediates and transition states along the reaction pathway. Due to the limitations of computational facility, MP2 calculations are performed only for gas phase. To ascertain that the identified transition states connect the designated reactants and products smoothly, the intrinsic reaction coordinate (IRC) (Gonzalez &Schlegel 1989, 1990) calculations were carried out at the M06-2X level of theory. All the electronic structure calculations were done using Gaussian 16 (Frisch 2016)program package.

The reaction rate coefficient was predicted by employing kinetic and statistical thermodynamic package KiSThelP(Canneaux et al. 2014). The rate constants of the OH reactions were calculated in the temperature range of 278-1000K using variational transition state theory (VTST) with Wigner tunnelling corrections as implemented in the KiSThelP program package as given below in Equations 1 and 2. The Wigner tunnelling corrections have been included,

$$k^{CVT} = min_s\, k^{GT}(T,s) \quad (1)$$

$$k^{GT}(T) = \chi(T)\frac{\sigma k_B T}{h}\frac{Q^{TS}(T,s)}{N_A Q^R(T)} e^{\frac{-v^{++}}{k_B T}} \quad (2)$$

Here, $\chi(T) = 1 + \frac{1}{24}\left(\frac{hlm(v^*)}{k_b T}\right)^2$

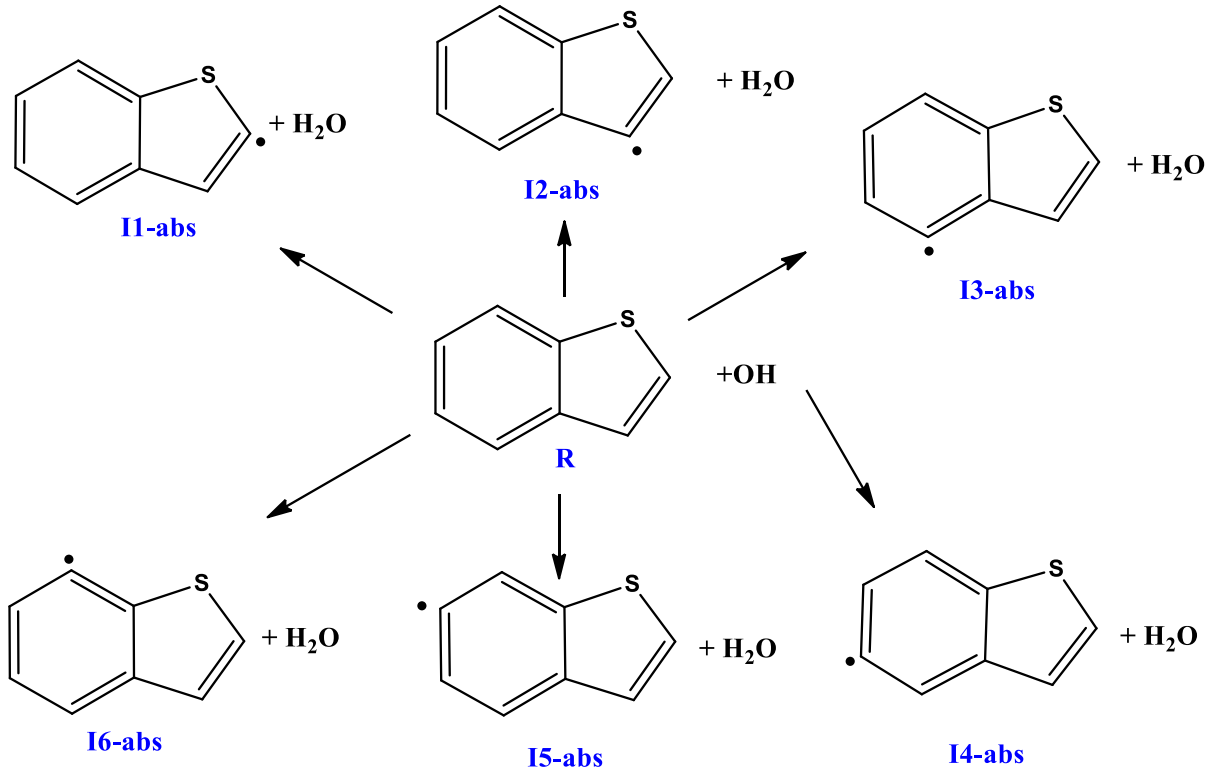
where, $\chi(T)$ is the tunnelling correction coefficient, σ is the reaction path degeneracy, k_B is the Boltzmann's constant, T is the temperature, h is the Planck's constant, $Q^{TS}(T)$ is the partition function of the transition state, Q^R (T) is the partition function of the reactants, and V^{++} represents the activation energy.

RESULTS AND DISCUSSION:

This manuscript examines three types of BT reactions involving OH radicals, HO_2, and H_2 through H-abstraction, OH addition, HO_2 addition, and desulfurization pathways, respectively. To assess the solvation effect of water, all four reaction types were examined in solvent phases using the M06-2X/6-311++G(d,p) level of theory. The detailed mechanistic pathways are presented in the following sub-sections.

1. BT WITH OH: H - abstraction channel

In atmosphere, the initial attack by the OH radical on BT can proceed via abstraction and/or addition pathways. The hydrogen abstraction reaction channel of BT +OH proceeds with six possible H-abstraction active sites as shown in Scheme 1. Investigation of individual reaction pathway has been carried out by means of Potential Energy Surface (PES) as displayed in Fig. 1. The complete set of reactions have been studied by characterizing the reactants (R), pre-reaction complexes (RCs), transition states (TSs), intermediate complexes (ICs) and products (Ps). The zero-point corrected (ZPE) energies and thermochemistry of all the H-abstraction pathways were calculated at M06-2X / 6-311++G(d,p) level of theory. Further, in order to evaluate the accurate energies, MP2/ 6-311++G(d,p) calculations have been carried out same level of theory.



Scheme 1: The proposed H-atom abstraction reactions of BT with OH radical.

The OH radical abstracts hydrogen atom of BT and gives a radical intermediate (I-abs) along with a water (H_2O) molecule. The potential sites of H-abstraction are C-H bonds

on the benzene ring; either α carbons C-H bonds adjacent to the thiophene ring or C-H bonds on the β-position of the thiophene ring. Scheme 1 depicts the pathway numberings of H-abstraction reactions which proceed via formation of a pre-reaction complex (RCs) in both gas and solvent phase. As shown in Fig. S1, various pre-reaction complexes (RC1, RC2, RC3, RC4) are encountered with corresponding binding energies of -5.55, -5.45, -5.43, -5.44 kcal/mol respectively via hydrogen bonding interaction between H atom of OH radical and C atom of thiophene ring below that of starting reactants. From Table 1, the H-abstraction takes place at C-H bonds on the benzene ring TS3 is the most favourable pathway with small relative energy barrier of 5.70 kcal/mol at M06-2X in gas phase, whereas the same pathway 3 is the most favourable reaction in solvent phase also with a relative energy barrier of 6.95 kcal/mol.

Similarly, the H-abstraction from benzene ring via transitions state TS4 and TS5 shows the relative energy barrier of 6.18 and 6.22 kcal/mol respectively in gas phase at M06-2X level of theory, whereas in solvent phase (water) the reaction barriers are slightly higher with an energy barrier of 7.01 and 7.09 kcal/mol, respectively. With no further dictations of numbers in Table 1, the order of the favourable reaction pathways is (from most to least favourable) Path 3, Path 4, Path 5, Path 6, Path 2 and Path 1.

Based on the DFT data's, all the proposed reaction pathways are exothermic and exergonic in nature. The order of the favourable reaction pathways obtained from the DFT results are in consistent with MP2 level of theory. From Table 1, we found the H-abstraction from C-H bonds on the β-position of the thiophene ring is less favourable due to lower reactivity than other bonds.

Table 1 Relative energy, enthalpy and Gibb's free energy (in kcal/mol) of initial H-abstraction reactions of BT with OH radical calculated at M06-2X (gas and water medium) and MP2/6-311++G(d,p) levels of theory.

	M06-2X						MP2 (gas phase)		
	Gas phase			Water medium					
	ΔE	**ΔH**	**ΔG**	**ΔE**	**ΔH**	**ΔG**	**ΔE**	**ΔH**	**ΔG**
R	0	0	0	0	0	0	0	0	0
RC1	-5.55	-4.42	-10.58	-4.52	-4.10	2.26	*	*	*
TS1-abs	8.73	6.13	14.21	9.98	7.30	15.47	35.77	38.53	37.38
IC1-abs	-4.27	-2.44	2.59	-3.78	-1.99	2.77	3.54	4.60	3.40
I1-abs	-0.78	-0.28	-1.43	-2.04	-1.58	-2.72	20.52	25.75	31.54
TS2-abs	7.30	4.71	12.77	8.57	5.87	13.76	33.75	35.20	33.94
IC2-abs	-6.59	-4.72	1.17	-5.70	-3.94	0.07	13.71	12.11	20.63
I2-abs	-2.29	-1.79	-2.91	-3.71	-3.24	-4.36	24.82	27.90	23.86
RC2- abs	-5.45	-4.40	-10.65	-4.58	-4.14	2.91	*	*	*
TS3-abs	5.70	3.12	11.22	6.95	4.30	12.38	23.59	26.46	25.32
IC3-abs	-9.59	-7.83	-1.68	-8.80	-7.14	-1.74	-5.84	-4.82	-0.37
I3-abs	-5.03	-4.66	-5.76	-6.51	-6.17	-7.25	10.41	8.10	16.40
TS4-abs	6.18	3.50	11.74	7.01	4.30	12.46	24.64	26.68	25.81
IC4-abs	-8.77	-7.16	-1.50	-8.65	-7.15	-2.59	10.52	8.20	16.60
I4-abs	-4.98	-4.75	-5.85	-6.61	-6.42	-7.51	17.87	22.66	28.74
RC3- abs	-5.43	-4.38	-10.77	-4.56	-4.14	2.89	*	*	*
TS5-abs	6.22	3.55	11.70	7.09	4.37	12.31	25.48	27.01	26.26
IC5-abs	-8.78	-7.14	-1.29	-8.66	-7.15	-3.13	19.71	24.14	20.04
I5-abs	-5.04	-4.83	-5.94	-6.63	-6.46	-7.55	23.23	26.11	24.93
RC4- abs	-5.44	-4.38	-10.86	*	*	*	*	*	*
TS6-abs	6.41	3.81	11.97	7.40	4.71	12.61	26.06	27.50	36.55
IC6-abs	-8.34	-6.65	-1.50	-8.46	-6.85	-1.38	17.39	21.98	28.20
I6-abs	-4.66	-4.31	-5.40	-6.16	-5.85	-6.93	23.29	26.11	25.04

*denotes non-converged entities

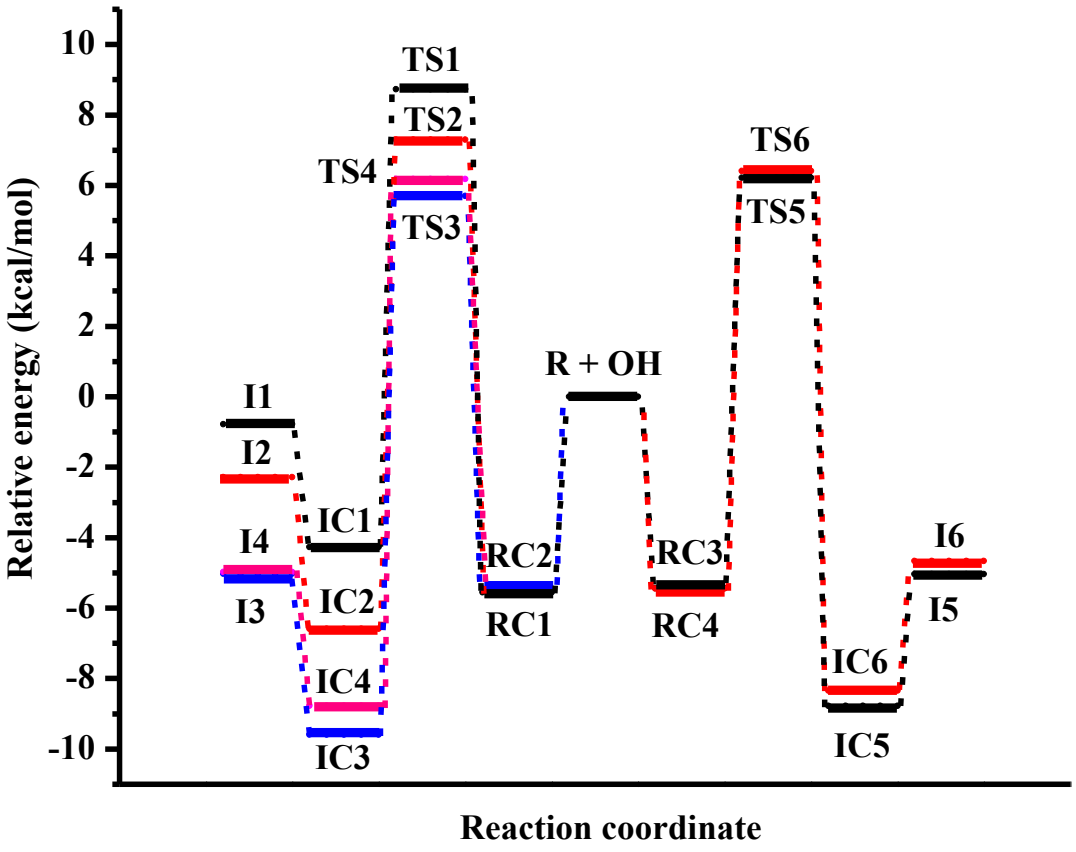
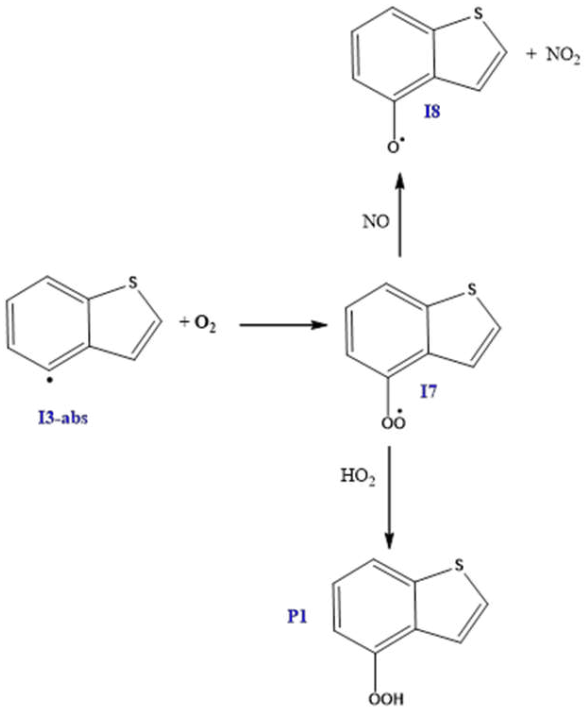


Fig. 1 The Potential Energy Surface (PES) of initial H-abstraction reactions of BT with OH radical calculated at M06-2X/6-311++G(d,p) level of theory. (Note: For Clear reading, energy levels are named as RC1, not as RC1-abs)

1a. SECONDARY REACTIONS: Reaction of I3-abs with O_2, HO_2 and NO oxidants

The intermediate I3-abs of the most favourable H-abstraction reaction further undergoes secondary reactions with O_2, NO and HO_2 atmospheric oxidants which is depicted in Scheme 2. The secondary reactions of BT radical (I3-abs) begin with the addition of O_2 to form a peroxy radical (I7) by means of barrierless reaction, as shown in relative energy profile Fig. 2. Then, the peroxy radical (I7) reacts with NO to formulate the alkoxy radical along with nitrate (RO + NO_2) (I8) via a barrierless and exothermic reaction. The optimized structures are shown in Fig. S2.



Scheme 2: Secondary reaction mechanism of I3-abs with O_2, NO and HO_2 radical.

Table 2: Relative energy, enthalpy and Gibb's free energy (in kcal/mol) of secondary reactions of I3-abs calculated at M06-2X and MP2/6-311++G(d,p) level of theory.

	M06-2X			MP2		
	ΔE	**ΔH**	**ΔG**	**ΔE**	**ΔH**	**ΔG**
I3-abs + O_2	0	0	0	0	0	0
I7	-45.92	-44.77	-40.84	-66.85	-67.94	-62.31
I7 + NO	0	0	0	0	0	0
I8	-32.61	-32.40	-32.30	-9.82	-10.29	-10.70
I7 + HO_2	0	0	0	0	0	0
TS7	2.41	-0.14	0.20	0.57	-0.17	-0.11
P1	-22.58	-24.59	-35.15	-9.35	-7.27	-3.25

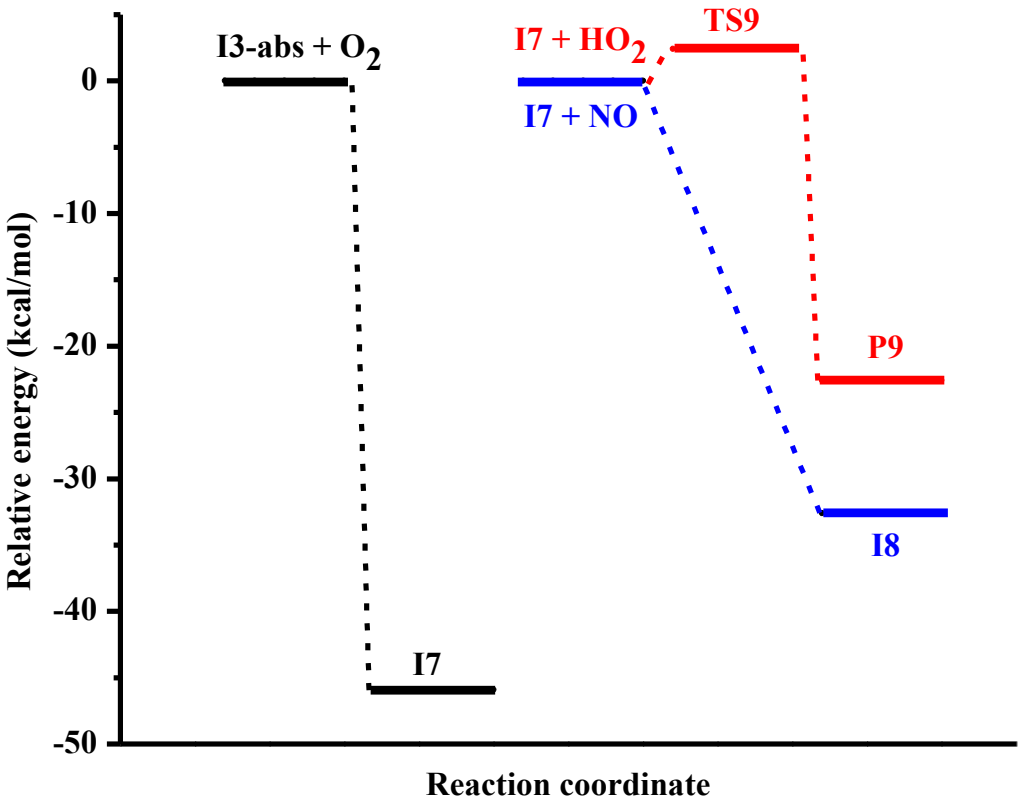
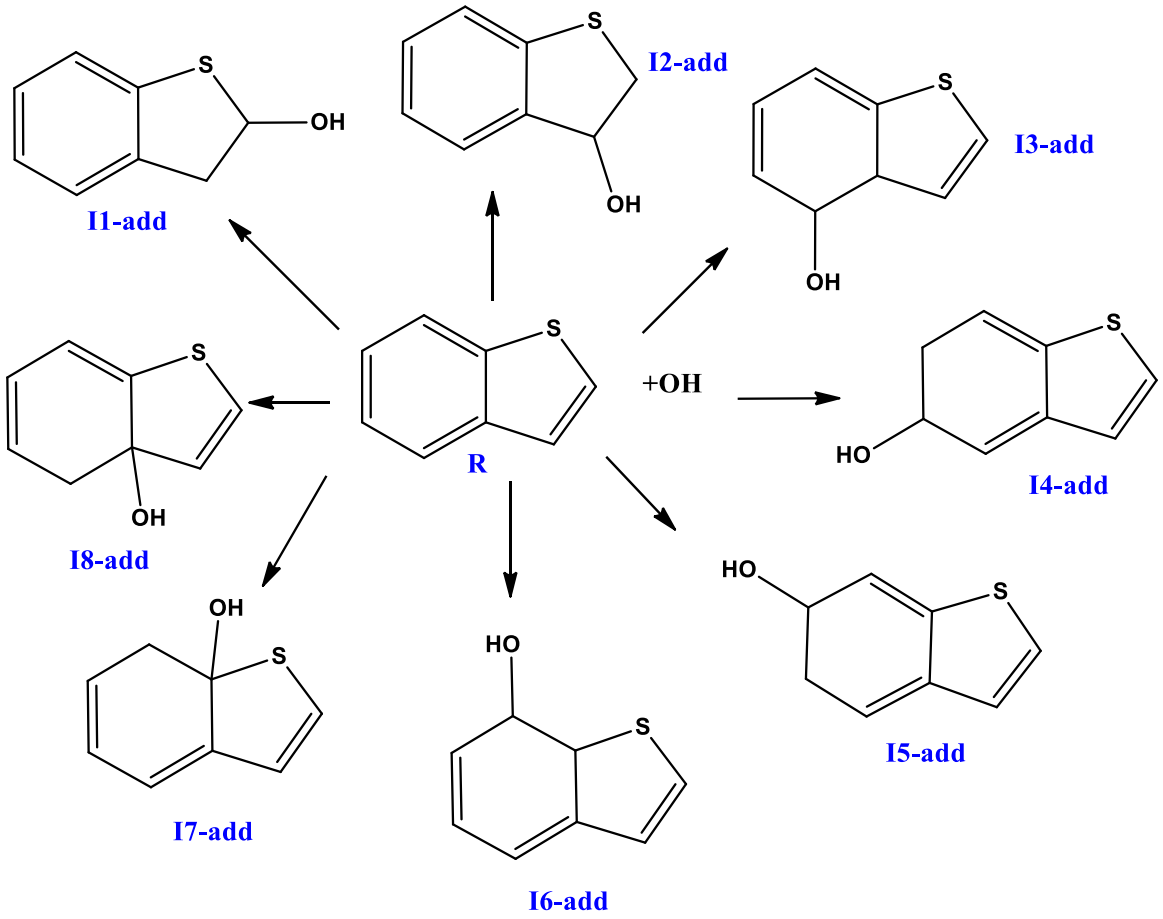


Fig. 2 The Potential Energy Surface (PES) of secondary reactions of intermediate I3-abs calculated at M06-2X/6-311++G(d,p) level of theory.

Despite the reaction of peroxy and nitrate formation, the peroxy radical (I7) reacts with HO_2 to form the hydroperoxide (P1) product through a transition state TS7 with a small energy barrier of 2.41kcal/mol at M06-2X level of theory. The thermochemical parameters listed in Table 2 depicts that all the three proposed secondary reactions are feasible through barrierless and exothermic reactions to form a stable product, except pathway 9.

2. ADDITION CHANNEL: BT with OH and HO_2

There are eight possible active sites for addition reactions for both OH and HO_2 (hydroperoxyl radical) with BT, due to the presence of the delocalized π electron cloud around the benzene and thiophene rings. The proposed eight addition pathways of BT are represented in Schemes 3 (OH) and 4 (HO_2), respectively. The optimized structures are shown in Fig. S3.



Scheme 3: The proposed OH addition reaction mechanism of BT.

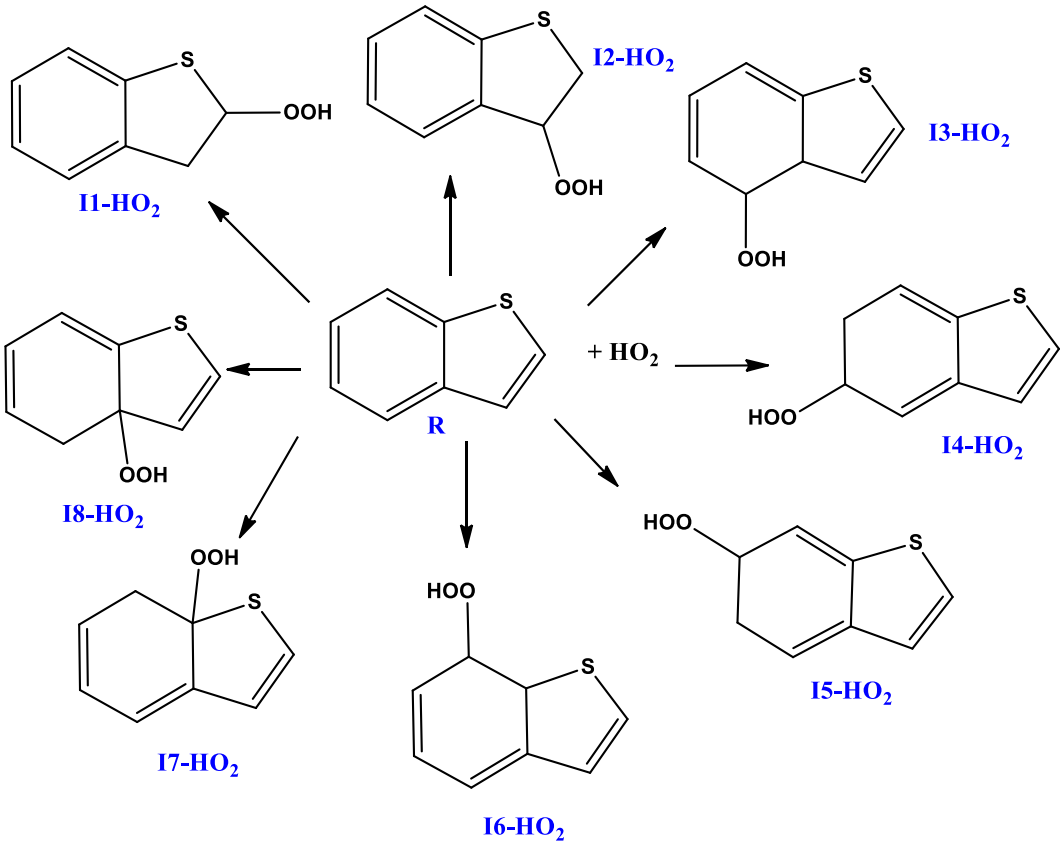
The study of addition reaction channel of BT with OH and HO_2 is important because the addition of OH and HO_2 radical takes place at both benzene and thiophene rings. At the entrance reaction channel, the formation of pre-reactive complexes (RCs) occurs without any energy barriers in both radical attacks as well as in gas, solvent phases. various pre-reaction complexes (RC1, RC2, RC3, RC4 and RC5) are encountered with corresponding binding energies of -5.55, -5.45, -5.37, -5.44 and -5.54 kcal/mol respectively via hydrogen bonding interaction between H atom of OH radical and C atom of thiophene ring below that of starting reactants. In HO_2 channel, three pre-reactive complexes are formed namely RC1-HO_2, RC2-HO_2 and RC3-HO_2 as shown in Fig. S4.

Table 3: Relative energy, enthalpy and Gibb's free energy (in kcal/mol) of OH-addition reactions of BT calculated at M06-2X (gas and water medium) and MP2/6-311++G(d,p) level of theory.

	M06-2X						MP2 (gas phase)		
	Gas phase			Water medium					
	ΔE	ΔH	ΔG	ΔE	ΔH	ΔG	ΔE	ΔH	ΔG
R	0	0	0	0	0	0	0	0	0
RC1-add	-5.55	-4.41	2.16	-4.52	-4.10	2.26	*	*	*
TS1-add	-2.48	-1.73	7.45	-2.13	-1.43	7.40	30.10	33.15	43.03
I1-add	-31.38	-28.96	-19.37	-31.26	-28.77	-19.12	-4.70	-1.22	8.58
TS2-add	-2.51	-1.69	7.30	-2.42	-1.61	7.23	30.14	34.13	43.89
I2-add	-24.61	-22.15	-13.03	-24.27	-21.72	-12.45	-21.47	-19.10	-9.76
RC2-add	-5.45	-4.40	1.94	-4.58	-4.14	2.91	*	*	*
TS3-add	-1.51	-0.75	8.24	-1.23	-0.47	8.54	30.19	33.84	43.67
I3-add	-22.94	-20.75	-11.39	-22.68	-20.40	-10.96	1.05	4.53	13.98
TS4-add	-0.13	0.72	9.97	0.07	0.89	10.02	32.63	36.10	45.86
I4-add	-16.58	-14.52	-5.15	-16.45	-14.35	-5.01	9.50	13.01	22.25
RC3-add	-5.37	-4.39	1.72	-4.56	-4.14	2.89	*	*	*
TS5-add	-0.61	0.22	9.43	-0.43	0.39	9.50	32.19	35.59	45.31
I5-add	-19.62	-17.51	-8.08	-19.49	-17.34	-7.96	6.28	9.42	18.73
RC4-add	-5.44	-4.39	1.84	-4.58	-4.14	2.91	*	*	*
TS6-add	-1.19	-0.34	8.92	-1.02	-0.22	8.73	30.15	33.95	43.94
I6-add	-21.53	-19.24	-9.78	-21.42	-19.05	-9.55	0.98	4.85	14.36
RC5-add	-5.54	-4.52	2.18	-4.52	-4.70	3.39	*	*	*
TS7-add	5.82	6.39	15.59	4.56	5.21	14.73	36.50	39.68	50.14
I7-add	-11.41	-9.78	2.15	-11.33	-9.64	0.30	14.92	18.09	28.38
TS8-add	4.81	5.45	15.14	4.60	5.28	14.92	35.56	39.12	49.56
I8-add	-6.94	-5.18	4.73	-5.88	-4.12	5.83	11.72	14.82	25.29

*denotes non-converged entities

The relative energies of the pre-reactive complexes RC1-HO_2, RC2-HO_2, RC3-HO_2 RC4-HO_2 and RC5-HO_2 are -7.55, -7.11, -7.57 -7.58 and -5.44 kcal/mol respectively at gas phase M06-2X level of theory. Among the possible addition reactions of OH channel, pathway 2 (TS2) is found to be the most favourable reaction with a relative energy barrier of -2.51 kcal/mol which occurs at the meta position of thiophene ring. Whereas, the OH addition at the ortho position of thiophene ring favours with a slightly higher relative energy barrier of -2.48 kcal/mol which lies within the accuracy range of the DFT calculations. On comparing all the eight OH addition reactions, pathway 7 and 8 are predicted to have higher energy barrier than the remaining six pathways as depicted in Table 3. The favourable order of OH addition reaction pathways are path 2 > path 1 > path 3 > path 6 > path 5 > path 4 > path 8 > path 7 in both medium and all the two level of calculations. Expectedly, all the reaction pathways were found to the exothermic and exergonic in nature.



Scheme 4: The proposed addition reaction mechanism of HO_2 with BT.

Table 4: Relative energy, enthalpy and Gibb's free energy (in kcal/mol) of addition reactions of BT with HO_2 radical calculated at M06-2X (gas and water medium) and MP2/6-311++G(d,p) level of theory.

	M06-2X						MP2 (gas phase)		
	Gas phase			Water medium					
	ΔE	ΔH	ΔG	ΔE	ΔH	ΔG	ΔE	ΔH	ΔG
R	0	0	0	0	0	0	0	0	0
RC1-HO_2	-7.55	-6.35	1.60	-5.44	-4.81	3.82	-7.99	-7.97	-0.31
TS1-HO_2	12.81	13.07	24.12	12.44	12.70	23.57	44.40	46.95	58.57
I1-HO_2	-5.29	-4.05	7.07	-4.49	-3.20	8.10	17.13	19.28	30.61
RC2-HO_2	-7.11	-6.53	2.87	-4.90	-4.29	4.14	-8.06	-7.93	-0.26
TS2-HO_2	12.13	12.58	23.71	12.34	12.81	24.02	41.75	45.61	57.51
I2-HO_2	-1.29	0.23	11.28	0.09	1.65	12.87	-1.74	-0.36	10.74
RC3-HO_2	-7.57	-6.34	1.65	-4.98	-4.42	3.24	-8.16	-7.94	-0.27
TS3-HO_2	21.78	21.73	33.81	21.44	21.41	33.50	48.76	51.75	64.46
I3-HO_2	18.54	19.13	30.96	18.60	19.21	31.09	34.00	36.46	48.71
RC4-HO_2	-7.58	-6.97	2.27	-5.39	-4.78	3.38	-7.99	-7.97	-0.32
TS4-HO_2	13.79	14.10	25.27	14.07	14.38	25.51	43.49	46.55	58.37
I4-HO_2	0.51	1.75	12.99	1.81	3.06	14.25	20.67	23.20	34.73
TS5-HO_2	17.00	17.28	28.51	17.17	17.44	28.58	47.83	50.72	62.42
I5-HO_2	6.74	7.85	18.86	7.84	8.97	20.17	29.31	31.87	43.00
TS6-HO_2	16.70	16.97	28.09	16.35	16.61	27.67	47.79	50.58	62.28
I6-HO_2	3.73	4.91	16.07	4.87	6.09	17.41	26.07	28.35	39.70
TS7-HO_2	15.11	15.45	26.91	14.58	15.00	26.55	44.56	47.80	59.88
I7-HO_2	2.06	3.32	14.59	2.71	4.04	15.53	20.75	23.73	35.35
RC5-HO_2	-5.77	-4.58	3.50	-4.32	-3.79	3.44	-8.06	-7.93	-0.24
TS8-HO_2	20.02	20.01	31.95	20.23	20.20	32.05	50.26	52.80	65.30
I8-HO_2	12.01	12.67	24.60	13.11	13.78	25.75	34.38	36.48	48.81

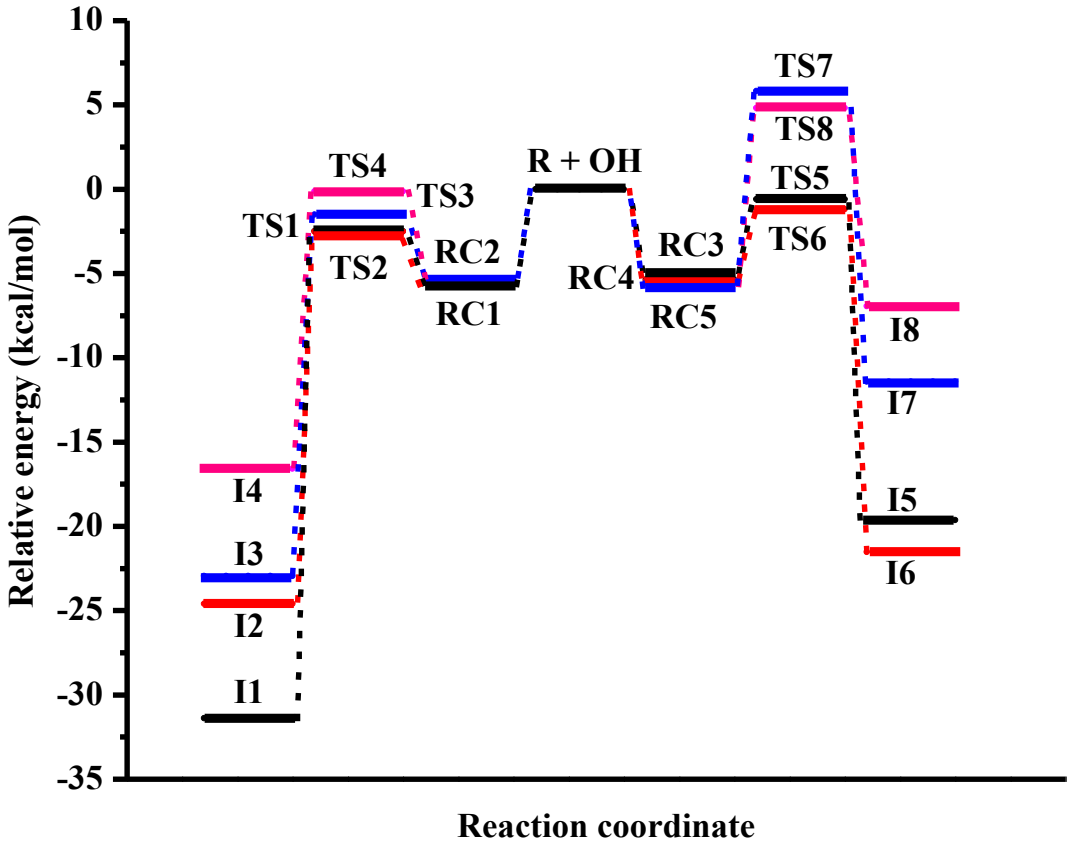


Fig. 3 The Potential Energy Surface (PES) of initial OH-addition reactions of BT with calculated at M06-2X/6-311++G(d,p) level of theory.

(Note: For Clear reading, energy levels are named as RC1, not as RC1-add)

The above Fig. 3 shows the potential energy profile of OH-addition reaction of BT. On the other hand, the most favourable HO_2-addition reaction takes place at same meta carbon position of thiophene ring with a relative energy barrier of 12.13 kcal/mol in gas phase at M06-2X level of theory. Similar to OH-addition channel, the second most favourable reactions occur at the ortho carbon position of thiophene ring. Based on the relative energy barriers shown in Table 4, the order of favour pathways is path 2 > path 1 > path 4 > path 7 > path 6 > path 5 > path 8 > path 3. In the solvent phase (water medium), the same meta carbon position remains the most favourable for HO_2 addition reaction and the similar favourable pathway order is found in all the three HO_2 addition channel electronic structure calculations. The Fig. 4 shows the potential energy profile of HO_2-addition reaction of BT.

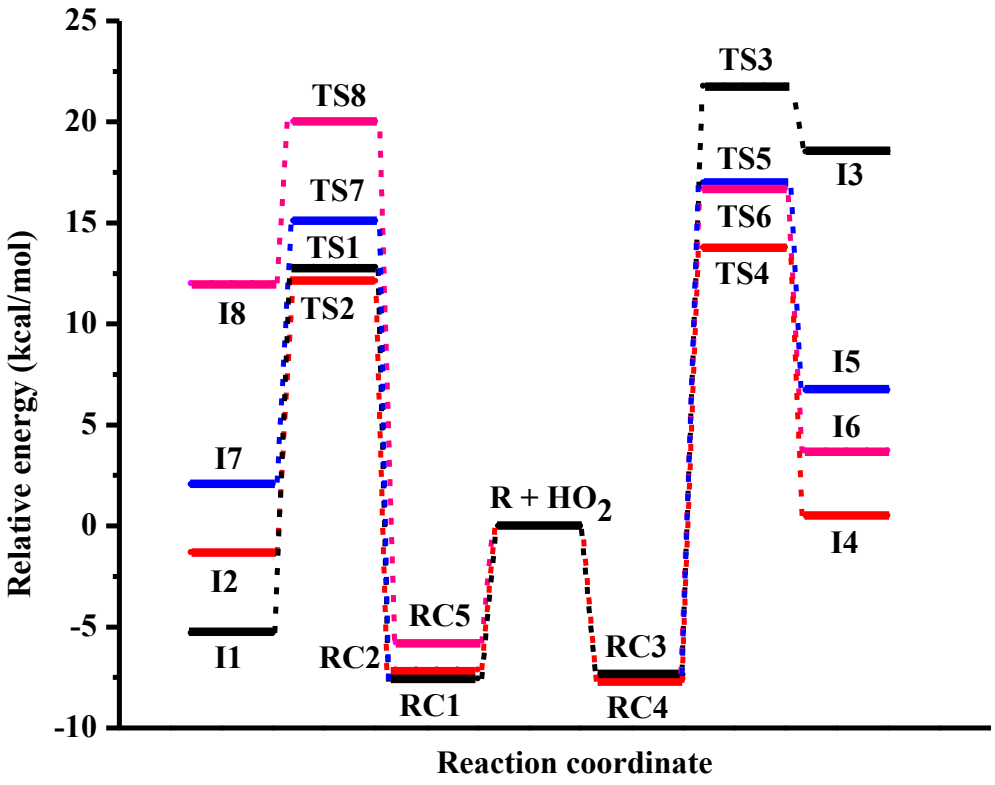
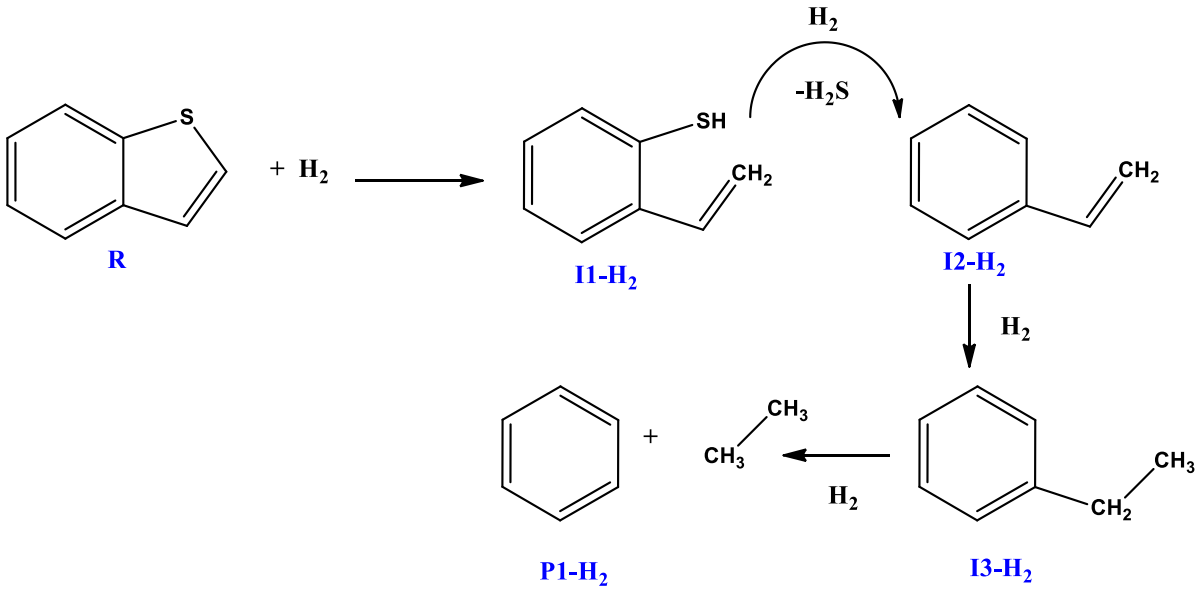


Fig. 4 The Potential Energy Surface (PES) of initial HO_2-addition reactions of BT calculated at M06-2X/6-311++G(d,p) level of theory.

(Note: For Clear reading, energy levels are named as RC1, not as RC1-HO_2)

3. AUTO-OXIDATION / DESULFURIZATION: BT with H_2

The auto-oxidation / desulfurization of BT with H_2 takes place via four step catalytic hydrogenations in which the addition of a hydrogen molecule (H_2) occurs at each step, as shown in Scheme 5. The corresponding optimized structures are shown in Fig. S5.



Scheme 5: The proposed desulfurization reaction mechanism of BT with H_2.

Initially, the formation of pre-reactive complex (RC1-H_2) is characterized as a barrierless and exothermic reaction with an relative energy of -1.40 kcal/mol.

(i) Hydrogenation: The addition of first hydrogen molecule occurs as a ring-opening reaction at the ortho position C-S bond of thiophene ring, the fused thiophene ring is partially hydrogenated and leads to the cleavage of C-S bond to form -SH and -CH_2 group. This ring hydrogenolysis leads to thiol intermediate (I1-H_2). **(ii) Desulfurization:** Further, the second protonation reaction step happens at the C-SH bond that leads to form the hydrocarbon intermediate (I2-H_2) along with a by-product of H_2S. As mentioned above, the formation of pre-reactive complex (RC2-H_2) is observed with a relative energy of -1.63 kcal/mol at M06-2X/6-311++G(d,p) level of theory. Therefore, the above-mentioned reactions are theoretically feasible and these reactions are well observed in the previous literature study on Theoretical study on the desulfurization mechanisms of thiophene and benzothiophene under inert and oxidative atmospheres by Fuli Zhang et.al(Zhang et al. 2020) in 2020. In gas phase, these two reaction pathways (TS1 and TS2) are characterized with considerably high energy barriers of 93.34 kcal/mol and 84.15 kcal/mol, respectively, whereas, in solvent phase, the barriers are

found to be 92.28 kcal/mol and 81.55 kcal/mol, respectively. On the other hand, the gas phase MP2 calculation predicts a reliable energy barrier of 59.49 kcal/mol and 64.95 kcal/mol for TS1 and TS2 respectively. The relative energy profile and the calculated relative energy values for the desulfurization reactions of BT with H_2 are shown in Fig. 5 and Table 5, respectively.

Table 5: Relative energy, enthalpy and Gibb's free energy (in kcal/mol) of desulfurization reactions of BT with H_2 calculated at M06-2X (gas and water medium) and MP2/6-311++G(d,p) level of theory.

	M06-2X						MP2 (gas phase)		
	Gas phase			Water medium					
	ΔE	ΔH	ΔG	ΔE	ΔH	ΔG	ΔE	ΔH	ΔG
R1 – H_2	0	0	0	0	0	0	0	0	0
RC1 – H_2	-1.40	-0.45	4.42	-1.46	-0.43	4.01	-19.21	-0.73	4.12
TS1 – H_2	93.34	92.13	100.65	92.28	91.05	99.58	59.49	78.56	87.11
I1 – H_2	-1.92	2.47	9.11	-2.57	1.80	8.23	-15.45	5.93	12.31
I1 + H_2	0	0	0	0	0	0	0	0	0
RC2 – H_2	-1.63	-0.60	4.53	-1.58	-0.44	5.25	-19.22	-0.65	4.56
TS2 – H_2	84.16	84.15	92.94	81.55	81.76	90.54	64.95	83.51	93.09
IC2 – H_2	-22.00	-17.80	-12.72	-21.82	-17.57	-11.84	-37.13	-15.46	-10.39
I2 – H_2	-16.58	-13.71	-16.81	-17.79	-14.84	-17.98	-13.29	-9.63	-12.21
I2 + H_2	0	0	0	0	0	0	0	0	0
RC3 – H_2	-1.49	-0.46	4.85	-1.43	-0.43	4.88	-35.79	-0.81	3.53
TS3 – H_2	32.38	36.36	45.84	*	*	*	*	*	*
I3 – H_2	-36.68	-30.04	-21.75	-35.97	-29.44	-20.91	-70.83	-29.73	-55.76
I3 + H_2	0	0	0	0	0	0	0	0	0
RC4 – H_2	-1.85	-0.79	5.03	-1.69	-0.64	5.19	-18.99	-0.48	4.85
TS4 – H_2	114.64	114.35	122.36	109.15	109.51	117.40	102.13	118.93	126.96
PC2 – H_2	-14.32	-9.00	-3.99	-14.02	-8.78	-4.02	-29.74	-6.77	-2.67
P1 – H_2	-11.49	-5.59	-30.41	-11.46	-5.54	-33.60	-26.11	-2.54	-24.74

*Denotes non-converged entities

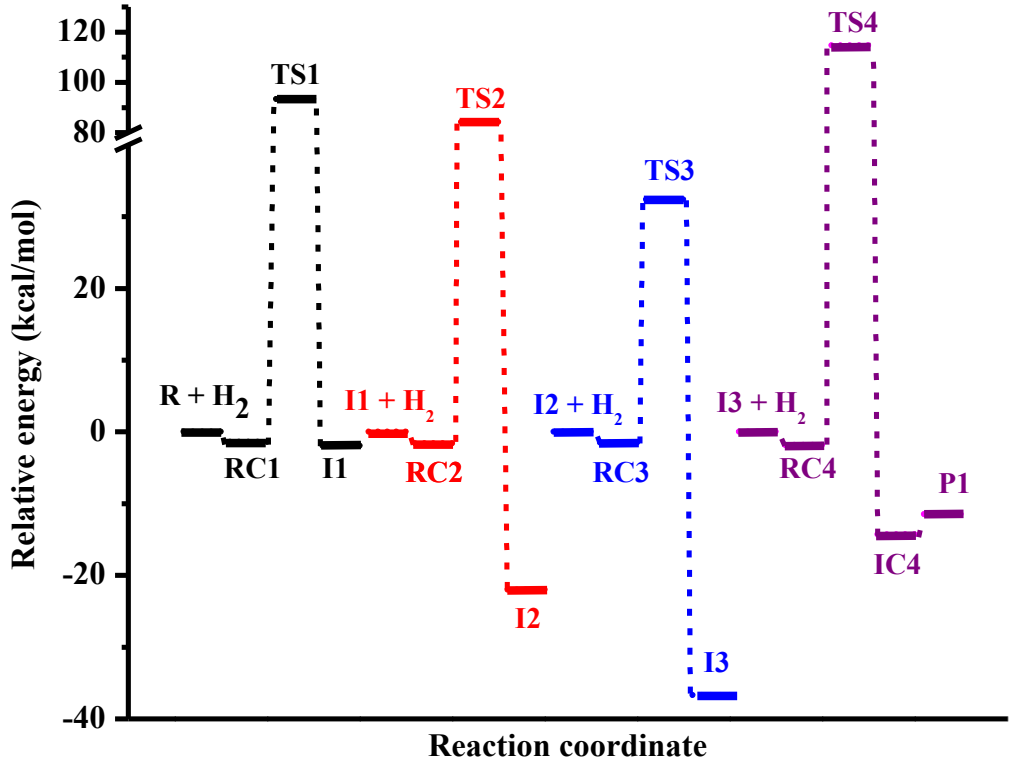


Fig. 5 The Potential Energy Surface (PES) of initial auto-oxidation / desulfurization reaction of BT calculated at M06-2X/6-311++G(d,p) level of theory.
(Note: For Clear reading, energy levels are named as RC1, not as RC1-H_2)

As a result of above two reaction steps, **(iii) Hydrogenation:** we ended with a hydrocarbon which further undergoes hydrogenation reaction from a pre-reactive complex (RC3-H_2) with a relative energy of -1.49 kcal/mol via transition state TS3 with an energy barrier of 32.38 kcal/mol in gas phase at M06-2X level of theory to form the intermediate I3-H_2 (ethylbenzene). **(iv) Hydrogenolysis:** The final reaction step is progressed through a pre-reactive complex (RC4-H_2) through a transition state TS4 with an energy barrier of 114.64 kcal/mol at M06-2X level of theory, to form a stable product ethane (C_2H_6), and benzene (C_6H_6). All the three electronic structure calculations [gas (114.64 kcal/mol) & solvent phase (109.15 kcal/mol) DFT and gas phase (102.13 kcal/mol) MP2] shows high energy barriers for transition state TS4 which may be due to cleavage of C-C bond associated with benzene ring. Besides the high energy barriers of the above-mentioned auto-oxidation / desulfurization of

BT, these reactions may play a vital role in petroleum refining and to reduce the sulfur content of fuels.

4. KINETICS: rate constants and branching ratio

Rate coefficient calculations are essential in determining the products and gaining insights into the dominant pathways for atmospheric oxidation reactions. The variational transition state theory (VTST) implemented in kinetic and statistical thermodynamic package (KiSThelP) was utilized to calculate the kinetics (rate co-efficient) for all OH radical reaction pathways. To predict the accurate kinetic parameters, Wigner's tunnelling co-efficient is included and calculated over the temperature range of 278 to 1000 K. Table 6 lists the predicted rate constants of H-abstraction channel which exhibits positive temperature dependence. The most favourable abstraction reaction pathway 3 is predicted to be kinetically more favourable than other reaction pathways. At room temperature, the gas phase rate constant of pathway 3 is calculated to be 2.30×10^{-14} cm^3 $molecule^{-1}$ s^{-1}, whereas the solvent (water medium) effect on kinetics is also studied at room temperature and the calculated value is 3.11×10^{-15} cm^3 $molecule^{-1}$ s^{-1}. It is noteworthy to mention that the reaction energy barrier has influenced the kinetics calculations and the outcome numbers.

On the other hand, the rate constants are calculated for OH addition reaction of BT and tabulated in Table 7. The rate constant of the favourable reaction pathway 2 is predicted to be 7.88×10^{-12} cm^3 $molecule^{-1}$ s^{-1} whereas the solvent phase rate constant is found to be 8.11×10^{-12} cm^3 $molecule^{-1}$ s^{-1} at room temperature 298 K. The temperature dependent rate constants of individual OH-addition reaction pathways are summed-up to find the overall rate constant for OH addition reaction of BT. The aforementioned individual rate constants are fitted into Arrhenius plot [1000/T vs Log(k)] as shown in Fig. 6 (H-abstraction) and Fig. 7 (OH addition), the three parameter Arrhenius equations are derived, as given below,

$$k_{H\text{-}abs} = 1.98 \times 10^{-10} \exp(-2462.4/T) \quad (3)$$

$$k_{OH\text{-}add} = 3.71 \times 10^{-11} \exp(-3178/T) \quad (4)$$

Surprisingly, as shown in Tables 6, 7 and Fig. 6, 7, the H-abstraction reaction of BT with the OH radical exhibits positive temperature dependence — that is, the rate constant increases with increasing temperature. In contrast, the OH addition reaction displays negative temperature dependence in the temperature range of 278–400 K. However, beyond 400 K, the rate constant for OH addition shifts and begins to exhibit positive temperature dependence. To strengthen the current finding's, recently *P. Arathala et al(Arathala &Musah 2024),* studied the gas phase oxidation of 3-Methyl-2-butene-1-thiol (MBT) with OH radical which explore that the OH addition reactions are favourable than H-abstraction reactions which exactly matches with our calculations.

Table 6: The rate constant (cm^3 $molecule^{-1}$ s^{-1}) calculated at VTST including Wigner tunnelling method for the initial H-abstraction reactions of BT with OH radical.

Temp (K)	I1-abs	I2-abs	I3-abs	I4-abs	I5-abs	I6-abs	Total
278	8.89×10^{-16}	1.11×10^{-15}	1.55×10^{-14}	6.26×10^{-15}	6.62×10^{-15}	4.36×10^{-15}	3.47×10^{-14}
288	1.33×10^{-16}	1.53×10^{-15}	1.94×10^{-14}	7.99×10^{-15}	8.48×10^{-15}	5.67×10^{-15}	4.32×10^{-14}
298	1.94×10^{-16} (2.35×10^{-17})	2.06×10^{-15} (3.73×10^{-16})	2.30×10^{-14} (3.11×10^{-15})	1.00×10^{-14} (2.65×10^{-15})	1.07×10^{-14} (3.47×10^{-15})	7.25×10^{-15} (2.25×10^{-15})	5.32×10^{-14} (1.19×10^{-14})
300	2.09×10^{-16}	2.18×10^{-15}	2.48×10^{-14}	1.05×10^{-14}	1.11×10^{-14}	7.61×10^{-15}	5.64×10^{-14}
400	3.44×10^{-15}	2.00×10^{-14}	1.21×10^{-13}	6.01×10^{-14}	6.53×10^{-14}	4.88×10^{-14}	3.19×10^{-13}
500	2.10×10^{-14}	8.65×10^{-14}	3.60×10^{-13}	1.96×10^{-13}	2.15×10^{-13}	4.32×10^{-14}	1.05×10^{-12}
600	7.74×10^{-14}	2.53×10^{-13}	8.24×10^{-13}	4.79×10^{-13}	4.31×10^{-13}	1.70×10^{-13}	2.11×10^{-12}
700	2.12×10^{-13}	5.90×10^{-13}	1.61×10^{-12}	9.81×10^{-13}	1.09×10^{-12}	9.11×10^{-13}	5.39×10^{-12}
800	4.79×10^{-13}	1.18×10^{-12}	2.82×10^{-12}	1.78×10^{-12}	1.00×10^{-12}	1.69×10^{-12}	8.95×10^{-12}
900	9.46×10^{-13}	2.12×10^{-12}	4.57×10^{-12}	2.97×10^{-12}	3.33×10^{-12}	2.86×10^{-12}	1.68×10^{-11}
1000	1.69×10^{-12}	3.51×10^{-12}	6.98×10^{-12}	4.65×10^{-12}	5.22×10^{-12}	4.53×10^{-12}	2.66×10^{-11}

() parenthesis values are at 298 K in water medium

Table 7: The rate constant (cm^3 $molecule^{-1}$ s^{-1}) calculated at VTST including Wigner tunnelling method for the initial OH-addition reactions of BT with OH radical.

Temp (K)	I1-add ($\times 10^{-12}$)	I2-add ($\times 10^{-12}$)	I3-add ($\times 10^{-12}$)	I4-add ($\times 10^{-14}$)	I5-add ($\times 10^{-13}$)	I6-add ($\times 10^{-13}$)	I7-add ($\times 10^{-18}$)	I8-add ($\times 10^{-18}$)	Total
278	6.85	8.59	1.62	7.47	1.98	4.98	3.06	7.19	1.78E-11
288	6.51	8.20	1.64	8.27	2.13	5.17	4.82	1.07×10^{-17}	1.72E-11
298	6.23 (6.26)	7.88 (8.11)	1.662 (0.94)	9.12 (7.69)	2.28 (1.86)	5.36 (6.82)	7.37 (2.96×10^{-17})	1.55×10^{-17} (2.13×10^{-17})	1.66E-11 (1.63E-11)
300	6.18	7.82	1.667	9.30	2.31	5.39	8.00	1.66×10^{-17}	1.65E-11
400	4.92	6.40	1.99	2.04×10^{-13}	4.13	7.62	1.85×10^{-16}	2.62×10^{-16}	1.47E-11
500	4.80	6.34	2.48	3.65×10^{-13}	6.53	1.04×10^{-12}	1.37×10^{-15}	1.53×10^{-15}	1.57E-11
600	5.11	6.81	3.11	5.82×10^{-13}	9.58	1.39×10^{-12}	5.66×10^{-15}	5.43×10^{-15}	1.80E-11
700	5.65	7.59	3.88	8.60×10^{-13}	1.33×10^{-12}	1.81×10^{-12}	1.65×10^{-14}	1.41×10^{-14}	2.12E-11
800	6.37	8.59	4.77	1.20×10^{-12}	1.78×10^{-12}	2.30×10^{-12}	3.86×10^{-14}	3.05×10^{-14}	2.51E-11
900	7.24	9.78	5.81	1.61×10^{-12}	2.31×10^{-12}	2.86×10^{-12}	7.75×10^{-14}	5.72×10^{-14}	2.97E-11
1000	8.24	11.40	6.98	2.10×10^{-12}	2.93×10^{-12}	3.51×10^{-12}	1.39×10^{-13}	9.75×10^{-14}	3.54E-11

() parenthesis values are at 298 K in water medium

Table 8: The branching ratio for the initial H-abstraction reaction pathways of BT with OH radical.

Temp (K)	I1-abs	I2-abs	I3-abs	I4-abs	I5-abs	I6-abs	Total
278	2.56	3.20	44.62	18.02	19.06	12.55	100.00
288	0.31	3.54	44.90	18.49	19.63	13.12	100.00
298	0.36 (0.20)	3.87 (3.14)	43.23 (26.19)	18.80 (22.31)	20.11 (29.22)	13.63 (18.94)	100.00 (100.00)
300	0.37	3.87	43.97	18.62	19.68	13.49	100.00
400	1.08	6.28	37.97	18.86	20.49	15.32	100.00
500	2.00	8.25	34.33	18.69	20.51	16.21	100.00
600	3.67	12.00	39.10	22.73	20.45	2.05	100.00
700	3.93	10.94	29.85	18.19	20.21	16.89	100.00
800	5.35	13.19	31.51	19.89	11.17	18.88	100.00
900	5.63	12.62	27.21	17.68	19.83	17.03	100.00
1000	6.36	13.21	26.26	17.49	19.64	17.04	100.00

() parenthesis values are at 298 K in water medium

Table 9: The branching ratio for the initial OH addition reaction pathways of BT.

Temp (K)	I1-add	I2-add	I3-add	I4-add	I5-add	I6-add	I7-add	I8-add	Total
278	38.417	48.175	9.085	0.419	1.110	2.793	0.000	0.000	100.000
288	37.931	47.778	9.556	0.482	1.241	3.012	0.000	0.000	100.000
298	37.469 (38.511)	47.392 (49.892)	9.996 (5.783)	0.548 (0.473)	1.371 (1.144)	3.224 (4.196)	0.000 (0.000)	0.000 (0.000)	100.000 (100.000)
300	37.387	47.308	10.085	0.563	1.397	3.261	0.000	0.000	100.000
400	33.493	43.569	13.547	1.389	2.812	5.187	0.001	0.002	100.000
500	30.610	40.431	15.815	2.328	4.164	6.632	0.009	0.010	100.000
600	28.435	37.894	17.306	3.239	5.331	7.735	0.031	0.030	100.000
700	26.713	35.886	18.345	4.066	6.288	8.558	0.078	0.067	100.000
800	25.400	34.252	19.020	4.785	7.098	9.171	0.154	0.122	100.000
900	24.340	32.880	19.533	5.413	7.766	9.615	0.261	0.192	100.000
1000	23.279	32.207	19.719	5.933	8.278	9.916	0.393	0.275	100.000

() parenthesis values are at 298 K in water medium

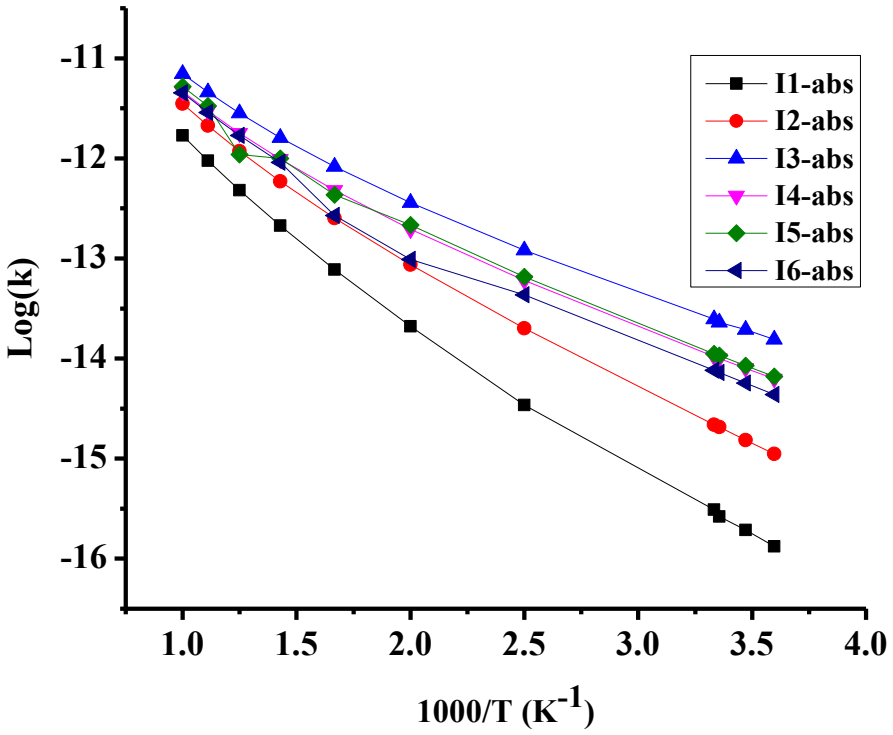


Fig. 6 The Arrhenius plot of H-abstraction reactions of BT calculated at M06-2X/6-311++G(d,p) level of theory.

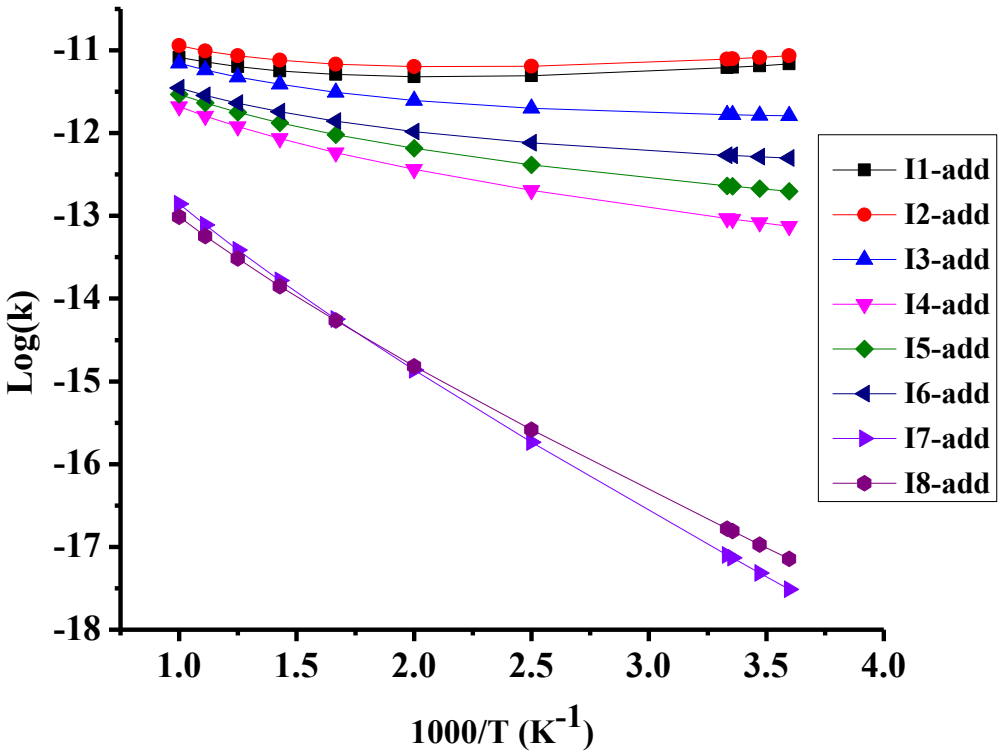


Fig. 7 The Arrhenius plot of OH-addition reactions of BT calculated at M06-2X/6-311++G(d,p) level of theory.

Further, to find the probability of each individual reaction of OH reaction channels, the branching ratios are calculated based on the predicted rate constants and tabulated in Table 8 and Table 9 for H-abstraction and OH-addition reactions, respectively. The branching ratio percentage (%) is determined by the ratio of the individual rate constant to the overall rate constant at a given temperature. Expectedly, the thermodynamically as well as kinetically favourable reaction pathways of both channels are predicted with higher probability i.e., Pathway 3 of H-abstraction possess 43.23% and Pathway 2 of OH-addition possess 47.39 % at 298K. It is noteworthy to point out that temperature dependent branching ratios of all the individual reaction pathways are found to be in agreement with the rate constants.

5. ATMOSPHERIC IMPLICATIONS and FUTURE STUDIES

In order to understand the complete atmospheric implications via the reaction properties of BT with OH radical, it is mandatory to calculate the atmospheric life-time of BT with respect to OH. The formula used to calculate the life time is

$$\tau_{OH} = \frac{1}{k_{OH}[OH]} \qquad (5)$$

Here, [OH] is the atmospheric concentration of OH radical(Atkinson et al. 2006) which was reported to be 1×10^6 molecules cm^{-3}. The life time of BT is predicted to be 0.69 days and 7 months with respect to OH addition and H-abstraction reactions, respectively.

To the best of our knowledge, there are no experimental or theoretical literature kinetics reports for the OH addition / abstraction reaction channel of BT. So, this is the first research work to disclose the individual and global rate constants. Since, there is absent of previous literature report, the calculated rate constants are compared with other same kind of similar research works of atmospheric OH radicals. Previous literature studies reported that OH addition favour the reaction mechanism than H-abstraction. One of the previous study from our research group, *B.Aazaad et al* investigated the OH channel reactions with 2,4,5 trimethylphenol (2,4,5,TMP) and reported the favourable OH addition reaction rate constant

to be $1.89x10^{-11}$ cm^3 $molecule^{-1}$ s^{-1} at 298 K calculated at CVT/SCT (canonical variational transition state theory with small curvature tunnelling) theory.

Recently, *P. Arathala et al(Arathala &Musah 2024),* studied the gas phase oxidation of 3-Methyl-2-butene-1-thiol (MBT) with OH radical using MESMER (The Master Equation Solver for Multi-Energy well Reactions) kinetic code and reported the global (overall) rate constant to be 5.99×10^{-11} cm^3 $molecule^{-1}$ s^{-1} at 298 K. Here, the present study predicts the gas phase OH-addition rate constant to be $1.66x10^{-11}$ cm^3 $molecule^{-1}$ s^{-1} at 298 K and whereas, the solvent (water) phase OH-addition rate constant to be $1.63x10^{-11}$ cm^3 $molecule^{-1}$ s^{-1} at 298 K. On comparing the aforementioned kinetics data of the similar research literatures (Mano Priya &Aazaad 2023), the present study predicts the same order ($x10^{-11}$) which validates our current findings. Besides, the current study has the limitations over the kinetics. Due to the computational cost, the kinetic calculations are carried out only for OH radical channel. However, the kinetics of HO_2 and H_2 pathways are considered to be important for the complete understanding of BT, which will be carried out in our future research.

CONCLUSION:

The current study unveils the important atmospheric abstraction / addition / auto-oxidation reactions of BT with OH, HO_2 and H_2 using density functional theory (DFT) at M06-2X/6-311++G(d,p) level of theory. The OH channel undergoes both H-abstraction and OH addition reactions and predicted that the favourable pathways are Path 3 (H-abstraction) and Path 2 (OH addition). For the first time, this study reveals the kinetics of BT reactions with OH radical and the calculated values are well-matched with the similar kind of reactions. The aforementioned rate constants are used to find the branching ratios of each individual pathway and followed by the atmospheric life time of BT with respect to OH radical atmospheric concentration using the overall rate constants. Further, the HO_2 addition and auto-oxidation reaction of BT with H_2 are investigated to find the possible routes for the

desulfurization end products of BT which are benzene and ethane. Based on all the aforementioned novel findings, this study delivers valuable insights of BT reaction channel which will be of great interest and significantly enlightens the understandings of atmospheric chemistry.

REFERENCES

Aazaad B, Lakshmipathi S (2018): OH initiated oxidation mechanism of monoterpene (linalool) – A first comprehensive theoretical study. Atmospheric Environment 189, 235-243

Algso MAS, Kivrak A, Konus M, Yilmaz C, Kurt-Kizildoğan A (2018): Synthesis and biological evaluation of novel benzothiophene derivatives. Journal of Chemical Sciences 130, 1-11

Arathala P, Musah RA (2024): Theoretical Insights into the Gas-Phase Oxidation of 3-Methyl-2-butene-1-thiol by the OH Radical: Thermochemical and Kinetic Analysis. The Journal of Physical Chemistry A 128, 2136-2149

Atkinson R, Baulch DL, Cox RA, Crowley JN, Hampson RF, Hynes RG, Jenkin ME, Rossi MJ, Troe J, Subcommittee I (2006): Evaluated kinetic and photochemical data for atmospheric chemistry: Volume II – gas phase reactions of organic species. Atmos. Chem. Phys. 6, 3625-4055

Canneaux S, Bohr F, Henon E (2014): KiSThelP: A program to predict thermodynamic properties and rate constants from quantum chemistry results†. Journal of Computational Chemistry 35, 82-93

Claußnitzer J, Bertleff B, Korth W, Albert J, Wasserscheid P, Jess A (2020): Kinetics of Triphase Extractive Oxidative Desulfurization of Benzothiophene with Molecular Oxygen Catalyzed by HPA-5. 43, 465-475

Deng Q, Yu A, Zhang L, Meng X (2021): Divergent Construction of Benzothiophene-Fused N-Heterocycles via Stereotunable Three-Component Domino Reactions. The Journal of Organic Chemistry 86, 3860-3870

Frisch MJT, G. W. Schlegel, H. B. Scuseria, G. E. Robb, M. A. Cheeseman, J. R. Scalmani, G. Barone, V. Petersson, G. A. Nakatsuji, H. Li, X. Caricato, M. Marenich, A. V. Bloino, J. Janesko, B. G. Gomperts, R. Mennucci, B. Hratchian, H. P. Ortiz, J. V. Izmaylov, A. F Sonnenberg, J. L. Williams Ding, F. Lipparini, F. Egidi, F. Goings, J. Peng, B. Petrone, A. Henderson, T. Ranasinghe, D. Zakrzewski, V. G. Gao, J. Rega, N. Zheng, G. Liang, W. Hada, M. Ehara, M. Toyota, K. Fukuda, R. Hasegawa, J. Ishida, M. Nakajima, T. Honda, Y. Kitao, O. Nakai, H. Vreven, T. Throssell, K. Montgomery Jr., J. A. Peralta, J. E. Ogliaro, F. Bearpark, M. J. Heyd, J. J. Brothers, E. N. Kudin, K. N. Staroverov, V. N. Keith, T. A. Kobayashi, R. Normand, J. Raghavachari, K. Rendell, A. P. Burant, J. C. Iyengar, S. S. Tomasi, J. Cossi, M. Millam, J. M. Klene, M. Adamo, C. Cammi, R. Ochterski, J. W. Martin, R. L. Morokuma, K. Farkas, O. Foresman, J. B. Fox, D. J. (2016): Gaussian 16 Rev. C.01, Wallingford, CT

Gonzalez C, Schlegel HB (1989): An improved algorithm for reaction path following. The Journal of Chemical Physics 90, 2154-2161

Gonzalez C, Schlegel HB (1990): Reaction path following in mass-weighted internal coordinates. The Journal of Physical Chemistry 94, 5523-5527

Herrera LC, Ramaley L, Grossert JS (2009): Fragmentation pathways of some benzothiophene radical cations formed by atmospheric pressure chemical ionisation. Rapid Commun Mass Spectrom 23, 571-9

Keri RS, Chand K, Budagumpi S, Balappa Somappa S, Patil SA, Nagaraja BM (2017): An overview of benzo[b]thiophene-based medicinal chemistry. European Journal of Medicinal Chemistry 138, 1002-1033

Kim I-K, Yoa S-J, Lee J-K, Huang C-P (2003): Reaction pathways and kinetic modeling for sonochemical decomposition of benzothiophene. Korean Journal of Chemical Engineering 20, 1045-1053

Li T, Li J, Zhang H, Sun K, Xiao J (2019): DFT Research on Benzothiophene Pyrolysis Reaction Mechanism. The Journal of Physical Chemistry A 123, 796-810

Lipparini F, Scalmani G, Mennucci B, Cancès E, Caricato M, Frisch MJ (2010): A variational formulation of the polarizable continuum model. The Journal of Chemical Physics 133, 014106-11

Mano Priya A, Aazaad B (2023): Mechanism and kinetics of atmospheric degradation of menthol initiated by hydroxyl radical. New Journal of Chemistry 47, 21490-21498

Marenich AV, Cramer CJ, Truhlar DG (2009): Universal Solvation Model Based on Solute Electron Density and on a Continuum Model of the Solvent Defined by the Bulk Dielectric Constant and Atomic Surface Tensions. The Journal of Physical Chemistry B 113, 6378-6396

Miertuš S, Scrocco E, Tomasi J (1981): Electrostatic interaction of a solute with a continuum. A direct utilizaion of AB initio molecular potentials for the prevision of solvent effects. Chemical Physics 55, 117-129

Prabhu MK, Louwen JN, Vogt ETC, Groot IMN (2025): Catalytic Hydrodesulfurization of Thiophene, Dibenzothiophene and 4,6-Dimethyldibenzothiophene on a CoMoS Catalyst. Catalysis Letters 155, 113 - 10

Qi W, Li Y, Liu Z, Li X, Jiang Y, Sun H (2020): Decomposition mechanism of thiophene compounds in heavy oil under supercritical water. Chemical Engineering Science 228, 115979-11

Scalmani G, Frisch MJ (2010): Continuous surface charge polarizable continuum models of solvation. I. General formalism. The Journal of Chemical Physics 132, 114110-16

Shen J, Yu A, Zhang L, Meng X (2020): Construction of benzothiophene fused pyrrolidone in water via a catalyst-free process and a mechanism study. Green Chemistry 22, 6798-6803

Yao X-Q, Li Y-W, Jiao H (2005): Mechanistic aspects of catalyzed benzothiophene hydrodesulfurization. A density functional theory study. Journal of Molecular Structure: THEOCHEM 726, 67-80

Zhang F, Guo H, Liu Y, Liu F, Hu R (2020): Theoretical study on the desulfurization mechanisms of thiophene and benzothiophene under inert and oxidative atmospheres. Fuel 280, 118683-8

Zhao Y, Truhlar DG (2008): The M06 suite of density functionals for main group thermochemistry, thermochemical kinetics, noncovalent interactions, excited states, and transition elements: two new functionals and systematic testing of four M06-class functionals and 12 other functionals. Theoretical Chemistry Accounts 120, 215-241

Declaration of competing interest

The authors declare that they have no known competing financial interests or personal relationships that could have appeared to influence the work reported in this paper.

Data availability

Data will be made available on request.

Authors' Contributions

Conceptual, Methodology, Validation, Writing original draft, Review & Editing – **Basheer Aazaad**, Conceptual, Methodology, Validation, Software, Review & Editing – **Angappan Mano Priya**

Acknowledgements, Funding, Ethical approval and consent to participate

This is not applicable.

Consent to Publish

All the authors give full consent to publish the manuscript.

Supplementary Files

This is a list of supplementary files associated with this preprint. Click to download.

- Authorresponsesheet.docx
- Supplementary.docx